

PCCP

Physical Chemistry Chemical Physics

Accepted Manuscript

This article can be cited before page numbers have been issued, to do this please use: S. Jensen, I. A. Løge, J. Bendix and L. Diekhöner, *Phys. Chem. Chem. Phys.*, 2024, DOI: 10.1039/D4CP00809J.



This is an Accepted Manuscript, which has been through the Royal Society of Chemistry peer review process and has been accepted for publication.

Accepted Manuscripts are published online shortly after acceptance, before technical editing, formatting and proof reading. Using this free service, authors can make their results available to the community, in citable form, before we publish the edited article. We will replace this Accepted Manuscript with the edited and formatted Advance Article as soon as it is available.

You can find more information about Accepted Manuscripts in the [Information for Authors](#).

Please note that technical editing may introduce minor changes to the text and/or graphics, which may alter content. The journal's standard [Terms & Conditions](#) and the [Ethical guidelines](#) still apply. In no event shall the Royal Society of Chemistry be held responsible for any errors or omissions in this Accepted Manuscript or any consequences arising from the use of any information it contains.

Cite this: DOI: 10.1039/xxxxxxxxxx

An approach for patterned molecular adsorption on ferromagnets, achieved via Moiré superstructures

Sigmund Jensen,^a Isaac Appelquist Løge,^{a,b} Jesper Bendix,^c and Lars Diekhöner^aReceived Date
Accepted Date

DOI: 10.1039/xxxxxxxxxx

www.rsc.org/journalname

We have used a Scanning Tunneling Microscope operated under ultrahigh vacuum conditions to investigate an oxo-vanadium-salen complex V(O)salen, that has potential applications as qubits in future quantum-based technologies. The adsorption and self-assembly of V(O)salen on a range of single crystal metal surfaces and nanoislands and the influence of substrate morphology and reactivity has been measured. On the close-packed flat Ag(111) and Cu(111) surfaces, the molecules adsorb isolated or form small clusters arranged randomly on the surface, whereas structured adsorption occurs on two types of Co nanoislands; Co grown on Ag(111) and Ag capped Co islands grown on Cu(111), both forming a Moiré pattern at the surface. The adsorption configuration can by Scanning Tunneling Spectroscopy be linked to the geometric and electronic properties of the substrates and traced back to a Co *d*-related surface state, illustrating how the modulated reactivity can be used to engineer a pattern of adsorbed molecules on the nanoscale.

Introduction

Molecules can play an important role as units in quantum information technologies,^{1–6} and molecular qubits have thus gained prominence due to their advantageous properties, including extended coherence times and potential operability at room temperature. Vanadyl complexes, where an oxo-vanadium(IV) ion is coordinated to organic ligands, present a compelling avenue for advancing molecular qubit technology.^{7,8} Notable coherence times have been reported for vanadyl-based qubits, indicating the stability of quantum information within these systems.^{9,10} However, integrating vanadyl complexes into existing quantum computing architectures or hybrid systems may pose challenges. One way of addressing this is to understand self-organization and surface patterning for deposited molecular systems. Square pyramidal oxo-vanadium(IV) complexes, have been successfully deposited on surfaces.^{11,12}

The vanadyl salen complex (Figure 1) is uncharged, very stable, and possesses a geometry suitable for surface deposition.

Bottom-up fabrication poses a suitable route for integrating vanadyl salen complexes in 2D geometries. The fundamental step for practical exploitation is to this end deposition and self-organisation of molecules on a suitable surface.^{13–15} Two approaches exist in obtaining ordered molecular layers on metallic substrates. Either the intermolecular interactions can be controlled by chemical functionalization^{16–18} or by engineering the substrate reactivity,^{19,20} to steer the molecules into ordered two-dimensional assemblies. The latter case is based on that different surface sites can have a variable reactivity, hence affecting the bonding affinities of molecules. Such an adsorption template can be obtained by introducing metallic adlayers with a lattice mismatch to the underlying crystal. Typically, this leads to Moiré patterns or reconstructions in the top surface layer that are accompanied by a modulated electronic structure with a periodicity of a few nanometers across the surface that can serve as a template for adsorption^{20–24}

By introducing ferromagnetic layers to the substrate, it is in addition to the lateral steering due to the modulation,

^a Department of Materials and Production, Aalborg University, Skjernvej 4a, 9220 Aalborg, Denmark. E-mail: ld@mp.aau.dk

^b Present address: Department of Chemical Engineering, Technical University of Denmark, Søtofts Plads 228A, 2800 Kgs. Lyngby, Denmark.

^c Department of Chemistry, University of Copenhagen, 2100 Copenhagen, Denmark.

† Electronic Supplementary Information (ESI) available: [details of any supplementary information available should be included here]. See DOI: 10.1039/b000000x/

also possible to use the exchange coupling in the vertical direction between the magnetic layer of the substrate and the magnetic moment of relevant metal-organic molecules. This can stabilize their magnetic properties against thermal fluctuations.^{25,26} Here we examine the bonding of molecules to Cobalt nanoislands, as these possess interesting spin-polarized surface states²⁷ and are easily grown on noble metal closed packed surfaces like Cu(111), Ag(111), Ir(111), Pt(111) and Au(111).^{21,25,28,29} Two combinations of Co islands are of particular interest. Namely the Co/Ag(111) and the Ag/Co/Cu(111) systems as the top surface layer of both surfaces reconstruct in a hexagonal Moiré superstructure, with the potential to steer the adsorption of molecules.^{21–23} The ability to steer the molecular adsorption for the two kind of cobalt island substrates is here examined by introducing a paramagnetic metal-organic molecule from the salen-family, seen in Figure 1.

The V(O)salen molecule is composed of a VO^{2+} unit, where the vanadyl ion is double bonded to an apical oxygen. This unit is incorporated in the square-planar-like bonding motif of the salen, meaning that VO^{2+} coordinates to two oxygen atoms and two nitrogen atoms all in the equatorial plane, yielding a total square-pyramidal five-fold coordination of a V(IV) ion.¹ The strong double bond to the apical oxygen is responsible for a d -orbital splitting leaving the d_{xy} orbital lowest in energy and singly occupied yielding a d^1 configuration.^{1,30} We adopt the nomenclature V(O)salen for the oxo-vanadyl-salen molecule and choose to examine this particular metal-organic complex partially due to its interesting magnetic properties, as the five-fold coordinated V(IV) ion has displayed quantum coherence detectable at room temperature, when this ion was incorporated in an organic structure related to the salen coordination motif.¹ In addition the salen class of molecules are interesting to examine on surfaces as the molecule exhibits an intramolecular dipole,^{16,18,31} which potentially can facilitate self-assemblies of molecular superstructures.^{20,32} Moreover the salen molecules are thermal resilient and can be sublimated under vacuum.

In this paper, we examine the adsorption behavior of V(O)salen on pristine Ag(111) and Cu(111), representing two flat, unmodulated substrates with identical symmetry of the atomic lattice, but with different reactivities. Then the adsorption behavior of the molecules on three different Cobalt island surfaces is addressed. First Co on Cu(111), which grows pseudomorphically. Then Co on Ag(111), where the Co layer reconstructs and forms an adsorption template with nm-scale periodicity and finally, the multilayer-system of Ag/Co/Cu(111), where a similar-sized template is formed, now with Ag in the top-

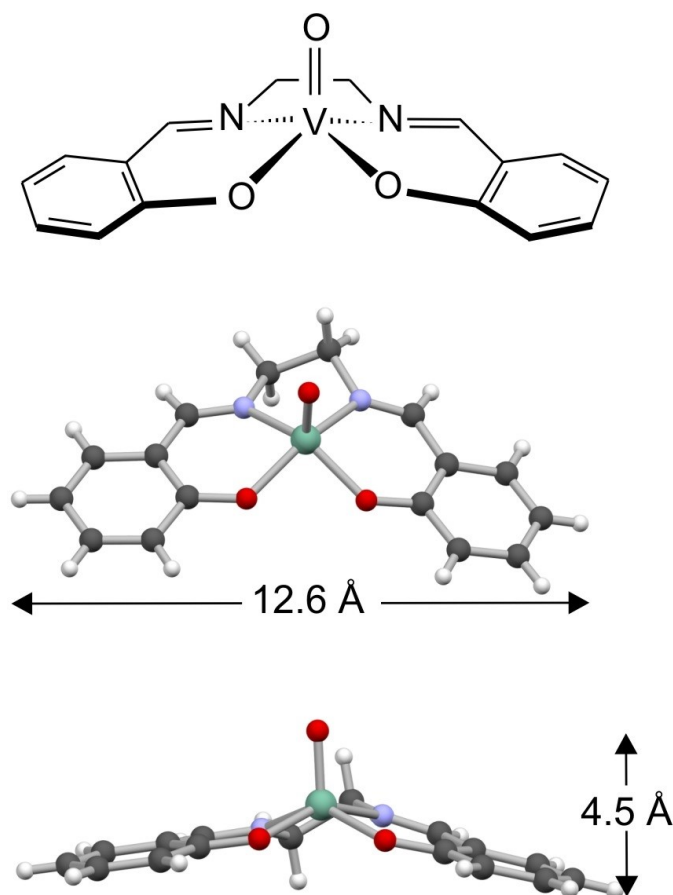


Fig. 1 Molecular structure and dimensions of V(O)salen [N,N'-bis(salicylidene)ethylenediamine]oxidovanadium(IV).

layer. Both the Co islands in the Co/Ag(111) and the bi-metallic Ag-Co islands in the Ag/Co/Cu(111) systems exhibit hexagonal reconstructions on the length scale of the molecules. The surface superstructures of the islands are imposing a spatial modulation of the local electronic structure, yielding both a geometric and an electronic template effect. We show how this can be used to obtain ordered adsorption of the V(O)salen molecules, and imply that engineering of surface superstructures can be a general approach to steer the adsorption behaviour of magnetic molecules on ferromagnetic templates.

Experimental

The experiments have been performed in ultra high vacuum (UHV) with a base pressure below 6×10^{-11} mbar using a Scanning Tunneling Microscope (STM), operated at low temperatures; 10 K for V(O)salen on Ag(111) and 77 K for the rest of the adsorption experiments on both Cu(111) and on the Cobalt islands. Single crystal Ag(111) and Cu(111) surfaces were cleaned by Ar^+ sputtering and subsequent annealing to ~ 800 K. Co and Ag were both introduced by thermal evaporation using an electron beam

evaporator. Ag was deposited on the Co/Cu(111) system to cap the Cobalt islands, and this was performed directly after the Co deposition and all depositions were performed with the substrate held at room temperature (RT). The V(O)salen molecule was synthesized according to literature methods³³ and purified by recrystallization from dichloromethane. Molecules were then introduced to Ag(111), Cu(111), Co/Ag(111) and Ag/Co/Cu(111) by means of thermal sublimation from a Knudsen cell evaporator with temperatures of 510 K. The local density of states (LDOS) of the surfaces was probed by Scanning Tunneling Spectroscopy (STS) performed at 77 K, where the differential conductance was acquired with a lock-in amplifier.

Results and Discussion

V(O)salen on Ag(111) and Cu(111)

V(O)salen was deposited on Ag(111) held at RT and then transferred to the STM operating at 10 K. Polymembered molecular clusters were observed as seen in Figure 2(a). When similar experiments were performed with the STM at 77 K or at RT, only fuzzy images evident of mobile diffusive molecules were observed. The motion of the molecules was effectively suppressed at 10 K. Tri-, four-, five-, and six-membered molecular clusters were observed, and originate from a self-assembling process, taking place during cooling to 10 K.

The tri- and four-membered clusters constitute 85 % of the observed assemblies at a molecular coverage of 0.08 ML, here defining this relative to the number of available adsorption sites and not the number of surface atoms, i.e. 1 ML coverage therefore means a close-packed layer of molecules filling the entire surface of the Ag(111) substrate. In the low coverage regime at 0.04 ML isolated molecules are also observed on the substrate and six different adsorption configurations are found, consistent with the substrate symmetry. At higher coverage ~ 0.3 ML, molecular aggregates with different shapes and sizes develop and the molecules clearly tend to interact with each other. We focus on the intermediate coverage regime of around 0.1 ML, where the ordered tri-, four-, five-, and six-membered molecular assemblies are most abundant. Interestingly, four enantiomeric tri-membered clusters exist as shown in the inset at the bottom of Figure 2(a), where they are labeled i, ii, iii, and iv. Here the salen shape of the molecules is identified and the apical oxygen ligand is weakly imaged as a protrusion in the center of the molecule. The triangular clusters i, iii, and ii, iv are congruent upon 180° rotation, whereas i, ii, and iii, iv are lateral inversions of each other. The larger assemblies consisting of four-, five-, and six-membered clusters can be derived

from the four enantiomeric tri-membered clusters, where additional molecules have formed intermolecular bonds to the outer part of the tri-membered unit, as displayed in the upper inset of Figure 2(a). From these observations we can derive two intermolecular bonding motifs of V(O)salen on the Ag(111) substrate, termed Open-Benzene-Center-, and Back-Back-interaction and display these schematically in Figure 2(c). Tri-membered clusters are stabilized by the open-benzene-center interaction, where the peripheral benzene part of one V(O)salen molecule points towards the equatorial oxygens of another molecule. The triangular unit is formed by three of these interactions and this type of intermolecular bonding is only available for the three inner molecules.

Four-, five-, and six-membered clusters form by further adopting a Back-Back bonding motif, where the additional molecules in the outer part of the assembly align its equatorial oxygens with the C₂H₄ bridge to either of the three inner molecules of the cluster (see right side of Figure 2(c)). Importantly, the V(O)salen molecules display an intermolecular bonding affinity on the Ag(111) substrate, which combined with the three-fold hexagonal symmetry of the Ag(111) surface yields three-fold symmetric assemblies on the substrate. The stability of the assemblies is limited though, and the intermolecular bonds are so weak, that when operating the STM at 77 K only mobile molecular entities are observed.

Similar experiments have been performed on the Cu(111) substrate. Again the sample was prepared at RT, with a molecular coverage of 0.09 ML V(O)salen, and transferred to the STM chamber. In this case the molecules were immobile on the substrate already at 77 K, which thus was used for all experiments on Cu(111). The result is displayed in Figure 2(b). 75 % of the molecules adsorb individually and, again, six different adsorption configurations can be observed consistent with the case of V(O)salen on Ag(111). These singly adsorbed molecular entities co-exist with molecules residing in both dimer and linear self-assembled clusters, as seen in the inset placed in the top right corner of Figure 2(b), where the salen shape and apical oxygen ligand again are clearly visible in the STM image. The molecules in the dimer formation are linked together via an intermolecular interaction termed the Closed-Benzene-Center bonding motif, where the benzene ring of one molecule points towards the center of another and vice versa. Only two molecules can be stabilized via this interaction, whereas larger linear clusters form by bonding more dimers together in a motif termed Head-Center bonding, as schematically shown in Figure 2(d). The linear clusters can be observed with different lengths, where the longest consists of six dimers. Moreover are the assemblies found

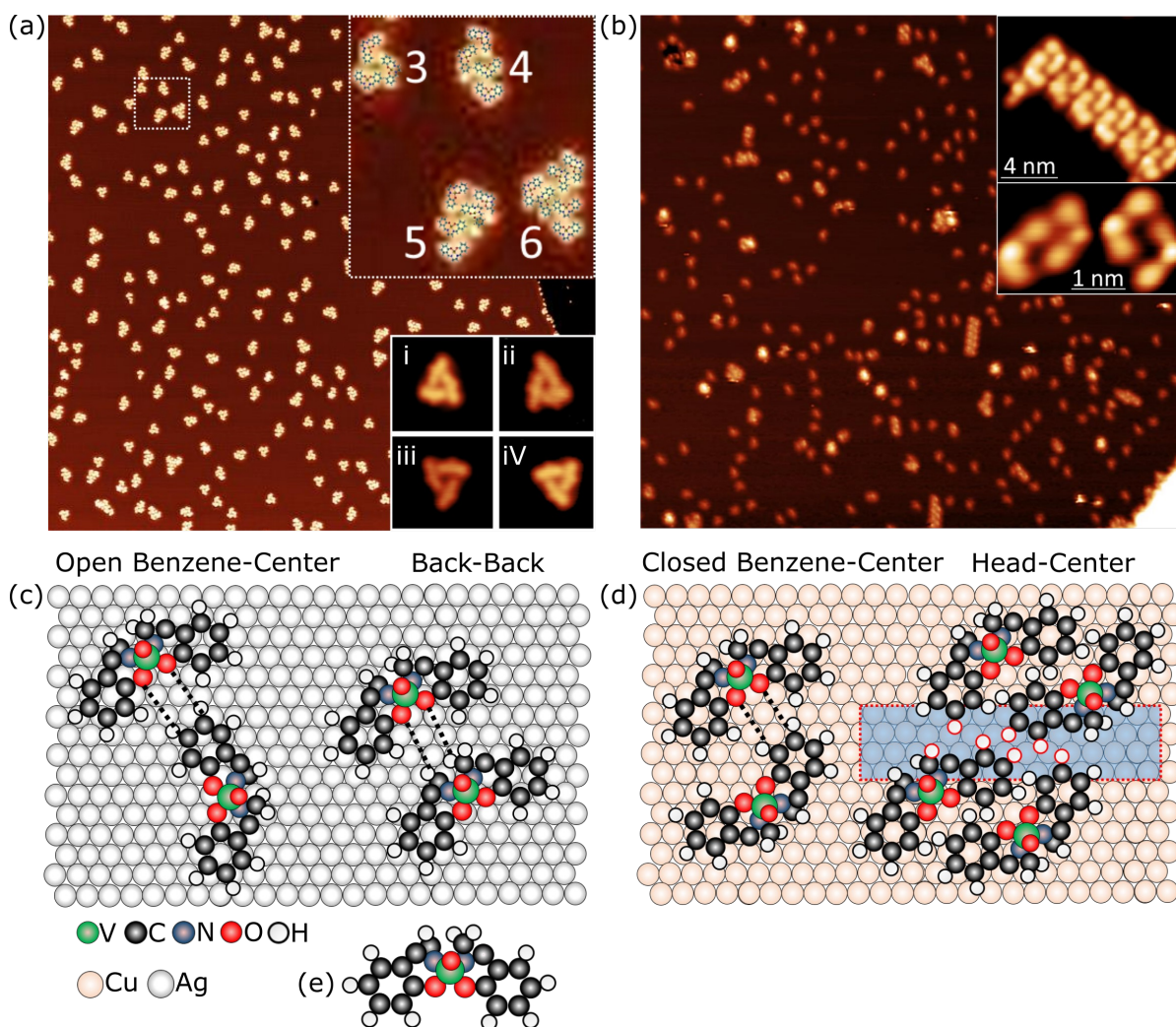


Fig. 2 (a) Self-assembled V(O)salen nanostructures on Ag(111). The zoom-in depicts the tri-, four-, five-, and six-membered clusters, with the molecular structure superimposed. Inset shows trimembered enantiomeric clusters, $4 \times 4 \text{ nm}^2$. ($I=0.32 \text{ nA}$, $V=408 \text{ mV}$, $100 \times 100 \text{ nm}^2$, 0.08 ML). (b) V(O)salen adsorbed on Cu(111), inset showing linear and dimer assemblies ($I=0.36 \text{ nA}$, $V=131 \text{ mV}$, $100 \times 100 \text{ nm}^2$, 0.09 ML). (c) and (d) Schematic of the Open-Benzene-Center, Back-Back, and the Closed-Benzene-Center, Head-Center intermolecular bonding motif on Ag(111) and Cu(111) respectively. The blue box is used to indicate that the interactions in the Head-Center motif is through multiple dipole interaction. (e) Ball model of the V(O)salen molecule.

rotated with 120° relative to each other, indicative of a substrate directed growth. At 0.4 ML the percentage of molecules singly adsorbed drop to 45% , since the formation of intermolecular bonds increases when more entities are present on the surface. V(O)salen is at the higher coverage present in either dimers, linear clusters or unordered molecular aggregates. Similar to V(O)salen adsorbed on Ag(111) the amount of molecules present in assemblies is delicately dependent on the coverage. Even though the triangular and linear clusters are significantly different, both formed assemblies are dictated by the three-fold symmetry of the (111) crystal facet. Furthermore we learn that V(O)salen displays an intermolecular bonding affinity and different molecular bonding motifs exist dependent on

whether it is adsorbed on Ag(111) or Cu(111).

The initial adsorption experiments on the pristine Ag and Cu crystals infer the delicate interplay between substrate-molecule and molecule-molecule interactions and show how the molecules are immobile at higher temperatures on the Cu surface compared to the Ag situation. On the other hand, V(O)salen is more likely to adsorb individually and self-assembled structures are therefore less frequently observed compared to the adsorption of V(O)salen on Ag(111) where the molecules are allowed to interact and are less perturbed by the substrate. Inspired by these observation we address the adsorption behaviour of V(O)salen on Moiré patterned Co nanoislands, having a periodicity in the surface superstructure on the length scale

of the molecules, in order to instigate a Moiré structure adsorption-template effect.

V(O)salen on Moiré templated Cobalt nanoisland

We now focus on the adsorption of V(O)salen on the modulated surfaces, first addressing the Co islands grown on Ag(111). Co was evaporated onto the Ag(111) substrate at RT, followed by transferring the sample to the STM operated at 77 K. In general we find the Co islands growing in 2-7 ML islands on the Ag(111) surface, consistent with previous STM studies.^{21,34} We measured adsorption and spectra on 3 ML Co islands. The Co islands exhibit three-fold symmetric shapes suggesting that Co attain its intrinsic hcp structure on the substrate and the Co island surface is the closed packed (0001) orientation. Hexagonal superstructures are revealed in the Co surface and can be traced back to a lattice mismatch between Co and Ag, resulting in a strain-induced Moiré pattern, as seen in Figure 3(a). Protrusions in the Co surface are observed at sites where Co atoms adsorb on top of Ag atoms yielding a 7×7 reconstruction with a hexagonal periodicity of ~ 2 nm.²¹ This local modulation of the Co surface geometry is accompanied by a modulation of the local electronic structure, as this is sensitive to the varying strain in the Co surface. To probe this, STS has been performed to measure the local density of states (LDOS) at three distinct sites of the Co islands on Ag(111), namely the fcc, the hcp and the on-top adsorption sites, marked by a yellow, red and blue crosses in Figure 3(e). The STS reveals a pronounced peak in the occupied part of the spectrum, which can be attributed to a d -like surface state.³⁴ The peak position relative to the Fermi level (E_F) varies with the different geometric sites, where the lowest appearing fcc sites show a peak in the LDOS at -200 mV whereas the peak is shifted to approximately -100 mV at the on-top sites. The peak position at the hcp sites is placed in between at approximately -130 mV, in accordance with the apparent height measured at the hcp position.

This effect can be rationalized in the d -band model, where Co atoms positioned in the depressions of the islands experience more compressive strain than Co atoms in the protrusions: The electrons tend to maintain a constant occupancy and to compensate for the extra electronic overlap in the most compressed sites, the d -band center is moved down in energy.³⁵ It is well established that the re-

activity of a transition metal surface is mainly governed by the valence d -electrons and that the affinity of the surface to bind molecules is affected by the surface strain. There exists an inverse relation between the strain in the surface and its reactivity, hence more compressed sites are generally less reactive than relaxed surface sites and this can be correlated back to a response of the metal d -band. The bond strength between the molecules and the metal is determined by the population of bonding and anti-bonding states, which is dependent on the position of the d -band center. As explained in the case of compressive strain, the d -band center will move down in energy yielding more anti-bonding states below E_F , hence populating these resulting in a weaker molecule surface bond.³⁶ Verification of the modulated LDOS and strain of the Moiré textured Co nanoisland will therefore also yield information of the local reactivity. From this reasoning it therefore should be expected that the less compressed on-top sites show a larger bonding affinity of the molecules, which is related to the energetic position of the d -peak being closest to E_F in these sites. This is expressed in the preferential adsorption behavior of V(O)salen as 90 % of 150 molecules from 10 different islands adsorb on-top of the corrugations, exemplified in Figure 3(a). Here molecules have been dosed at RT to a prepared Co/Ag(111) system and the sample was then transferred to the STM operated at 77 K. Molecules clearly reside on the protrusions in the Co island template and follow the hexagonal pattern in the surface superstructure. Some of the V(O)salen shape is recovered in the image as displayed in the inset of Figure 3(a), but generally they appear less distinct though, compared to the case of V(O)salen on Ag(111) and Cu(111) (Figure 2). This might be explained by the direct interaction between the molecule and the ferromagnetic Co layer, as adsorption of molecules on ferromagnetic supports have proven to significantly alter the electronic and magnetic properties of both surface and molecule, originating from the large reactivity of the substrate.^{25,37-41} It is a challenge though, to quantify the contribution from electronic and magnetic effects.

We now show that a similar ordered adsorption of the molecules can be obtained by engineering the surface of bilayer high Co islands grown on Cu(111), by capping these with a 1 ML Ag adlayer. Pure Co islands on Cu(111) grow pseudomorphically and to design an ordered adsorption template for V(O)salen on Co islands on Cu(111), Ag is added as an additional component, forming bi-metallic layered Ag-Co island heterostructures on the Cu(111) substrate.²³ This is performed by first depositing Co and then Ag to the Cu(111) substrate at RT, followed by a sample transfer to the STM operated at 77 K. Both directly on Cu(111)⁴² and on the Co-islands on Cu(111),²²⁻²⁴ Ag

* A small peak above the Fermi level is also observed at around +30meV. Since the reactivity and thus the molecular adsorption behavior, is mainly governed by the electronic structure below the Fermi level this has not been given further attention. One thing to note from ref³⁴ is though, that the degree of spin-polarization is vanishing for this peak, compared to the peak below E_F .

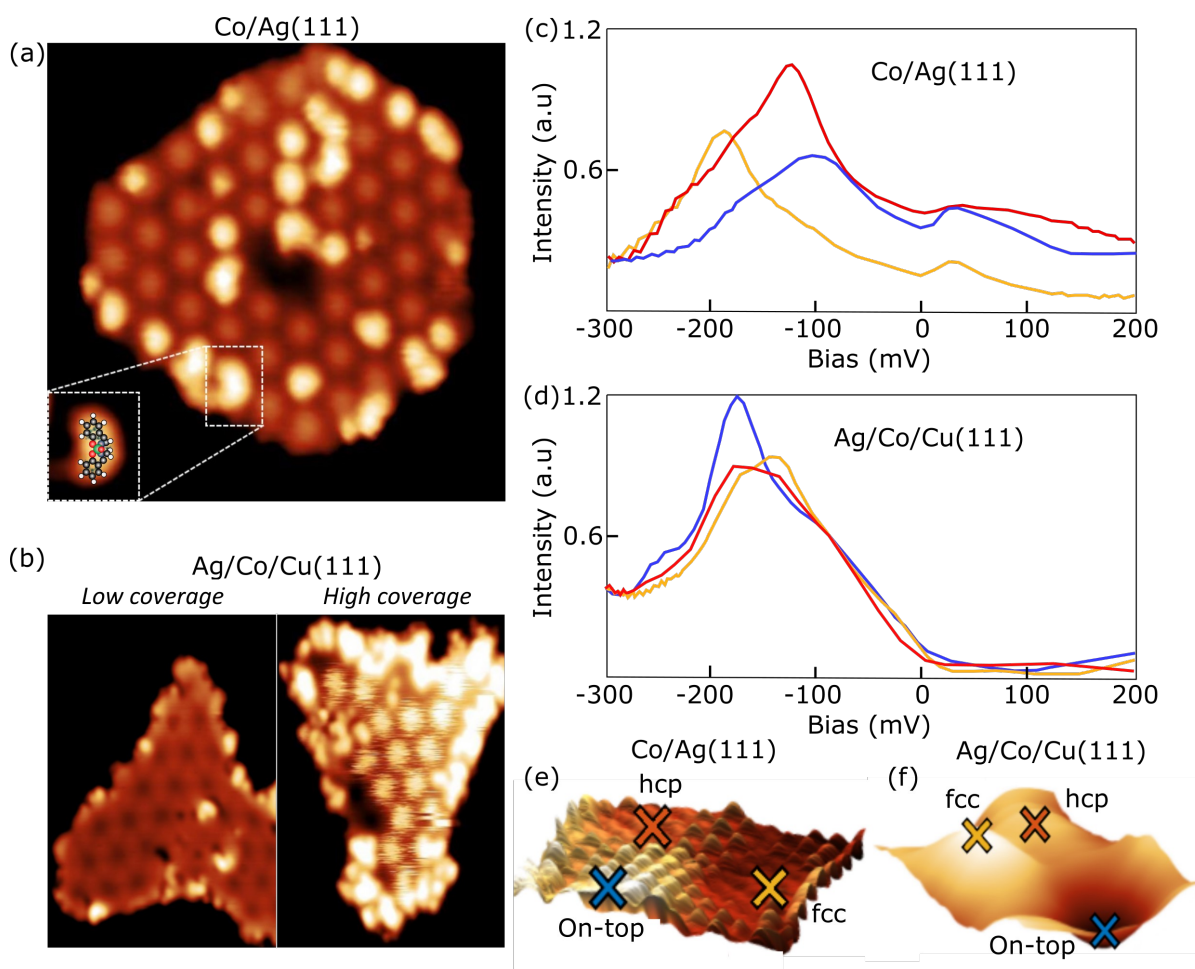


Fig. 3 (a) STM image showing the ordered adsorption of V(O)salen on the Moiré modulated surface of the 3 ML Co island grown on Ag(111). The inset highlights a V(O)salen molecule, with schematics of the molecule superimposed. ($I=0.32$ nA, $V=25$ mV, 30×30 nm²). (b) V(O)salen adsorbed on the Moiré modulated surface of the Bi-metallic 1 ML Ag- 2 ML Co island on Cu(111) at low and high coverage. ($I=0.35$ nA, $V=349$ mV, 20×30 nm² for each). (c) and (d) Point spectroscopy acquired at the on-top (blue), hcp (red) and fcc (yellow) sites of the modulated Co and Ag-Co surfaces. (e) and (f) High-resolutions STM images of the corrugation of the Co/Ag(111) ($I=0.32$ nA, $V=573$ mV) and Ag/Co/Cu(111) ($I=0.7$ nA, $V=442$ mV) surfaces respectively. All these spectra have been taken on clean 3 ML high islands without molecules.

forms hexagonal Moiré superstructures. This imposes a periodic structured surface as seen in the inset of Figure 3(b). Interestingly the surface d -state of Co can still be captured in STS, but the state is upshifted in energy with approximately 150 meV compared to the Ag uncovered case and consequently, the local electronic structure of the Co islands is periodically modulated with the period of the Ag Moiré lattice (Figure 3(b)).²² This is evident from the point spectroscopy displayed in Figure 3(d). The relation between the apparent heights of the Ag atoms adsorbed in the fcc, hcp and on-top sites on the Co islands is opposite to the Co/Ag(111) system, which can be realized by symmetry arguments (Figure 3(f)). Now fcc sites appear highest, followed by hcp sites and on-top sites²². STS reveals that the d -state positioned at the on-top site is lower

in energy, with a peak at -175 meV, compared to the hcp and fcc sites, showing pronounced peaks at -173 meV and -143 meV respectively. The relative position of the peaks can be attributed to a decreasing overlap between Co d - and Ag sp -states moving from the on-top to the fcc sites. This is thereby another example of a surface experiencing a varying strain, which modulates its LDOS and hence the local reactivity of the bi-metallic interface. In comparison the d -state of the Co islands on Ag(111) is shifted with 100 meV, possibly imposing a more pronounced electronic template effect on the local reactivity, than for the Ag capped Co islands on Cu(111), showing a less modulated LDOS.

After characterizing the Ag/Co/Cu(111) system molecules were deposited on the sample at RT and transferred to the STM. Again substrate-directed adsorption

was observed dictated by the hexagonal superstructure in the Ag-Co islands surface displayed in Figure 3(b). Here the Ag-Co island is completely covered with molecules, and the structure in the Ag-Co is difficult to see. In experiments performed with lower molecular coverage, the Ag superstructure is revealed and molecules preferentially reside on the protrusions at the fcc site, as seen in the inset of Figure 3(b). This is coinciding with the Co *d*-states being closest to E_F at these sites, as in the case for V(O)salen adsorbing in the on-top site of Co on Ag(111). The bi-metallic Ag/Co islands on Cu(111) and the Co islands on Ag(111) thereby share this molecule-template bonding motif. It should be mentioned that the difference in energy between the peak in the fcc and on-top sites for the Ag/Co islands is likely too small to completely explain the preferential adsorption behaviour of the molecules⁴³ and that bulk states not captured in the STS might also play an important role in the bond formation. Clearly this is the case for V(O)salen adsorbing on Co islands on Cu(111) as the Co *d*-surface states here are lower in energy compared to the surface state on the two other island substrates, which solely based on this emphasizes a lower reactivity for the former case.

V(O)salen on flat Cobalt nanoisland

V(O)salen molecules have additionally been introduced to the Co/Cu(111) substrate at RT, followed by a sample transfer to the STM operated at 77 K. Co was deposited onto Cu(111) at RT forming bilayer high pseudomorphic triangular shaped bilayer high Co nanoislands.^{44,45} The *d*-like surface state is similarly present on these Co islands, here at an energy of -300 mV.²⁷ The RT adsorption of V(O)salen was characterized by dissociation of the molecules and round bright spots with a significantly smaller size than V(O)salen were consistently seen on the surface (Figure 4(a) and (b)). Furthermore, a hydrogen adlayer (1H-(2×2)) was observed at the surface with a periodicity of 0.5 nm × 0.5 nm equivalent to that of hydrogen adsorbed on Co islands on Cu(111).^{46,47} Apart from the round molecular fragments and the H-adlayer, V(O)salen shaped protrusions were also found indicating that some of the V(O)salen molecules adsorb intact. This points towards a partial decomposition of some of the V(O)salen molecules on the reactive bilayer Co islands.⁴⁸ The brim of the V(O)salen is terminated with hydrogen, and it is therefore inferred that the H-adlayer originates therefrom. Lastly, it is noted that the adsorption of the intact V(O)salen molecules appears disordered as expected from a system where the molecule-surface bond dominates over the inter-molecular bonds.²⁰ In addition the flat struc-

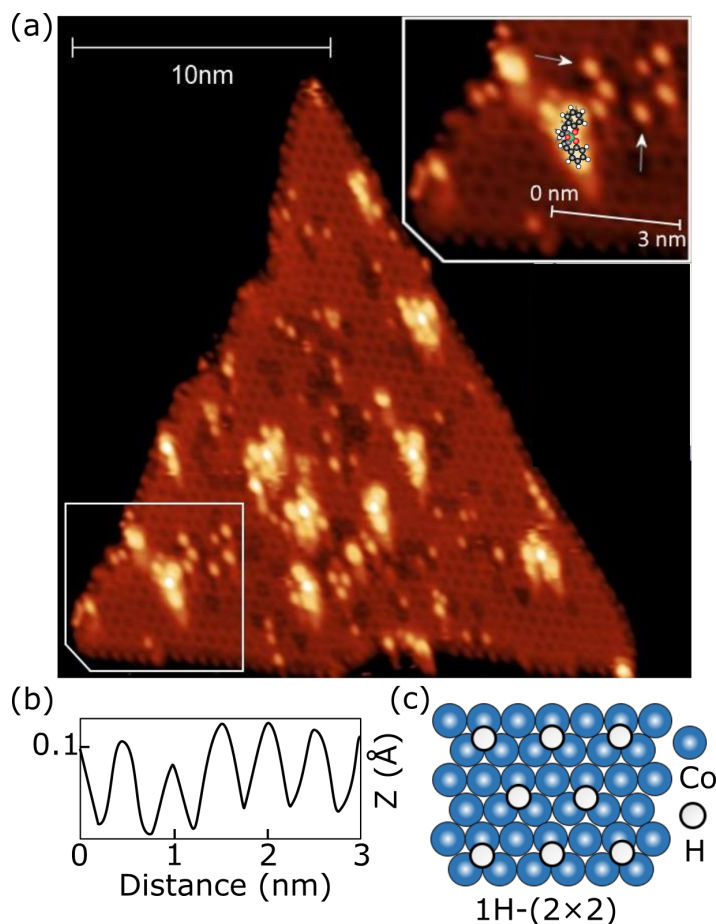


Fig. 4 (a) V(O)salen adsorbed on flat pseudomorphic 2 ML Co islands on Cu(111). The inset displays the lower left corner of the Co island where a V(O)salen shaped protrusion is identified, round fragments highlighted by white arrows, and H-superstructure on the Co surface are evident. (b) The apparent height analysis shows the periodicity of the H-adlayer. (c) Ball model of the 1H-(2×2) structure on the Co surface. ($I=0.39$ nA, $V=25$ mV, 30×25 nm²)

ture and unmodulated LDOS of the Co islands on Cu(111) does not invoke any molecular steering or periodic ordering.

V(O)salen on the modulated Ag/Co/Cu(111) template

When growing the modulated Ag-capped Co-islands on Cu(111) a mixed variety of island structures are found simultaneously on the surface as shown in the overview STM-image and ball models in Figure 5. First Co is deposited, forming triangular shaped bilayer high islands (area C). Then Ag is deposited resulting in 1 ML Ag/Cu(111) (area A) and 2 ML Ag/Cu(111) (area D). Note that the 2 ML Ag completely surrounds the bilayer high Co island. In addition some of the Co islands become capped with Ag (area B), that consist of 1 ML Ag/2 ML Co/Cu(111). All structures have been identified be-

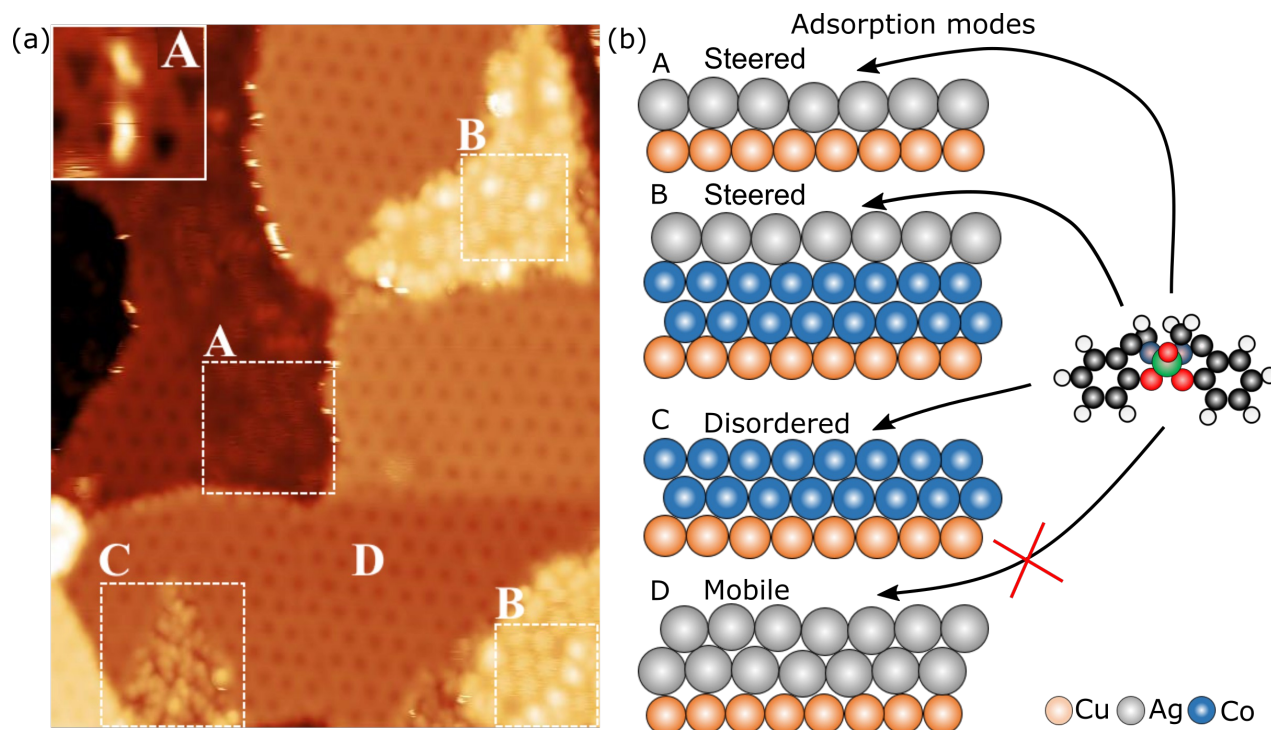


Fig. 5 (a) The Ag/Co/Cu(111) system, image displaying V(O)salen adsorbed on 1 ML Ag/Cu(111) (A), the Ag capped Co nanoislands (B), the bare Co surface (C) and the Ag bilayers on Cu(111) (D). ($I=0.35$ nA, $V=349$ mV, 40×65 nm²) Inset in the top right corner displays V(O)salen residing on the Ag monolayer in both a immobile and mobile fashion (fuzzy streaks), 3×4 nm². (b) Ball model of the different adsorption modes for V(O)salen on the Ag/Co/Cu(111) system.

fore depositing molecules from the geometry (apparent heights, reconstructions and Moiré structures) and from STS-spectra as described earlier.

On 1 ML Ag/Cu(111) (area A), V(O)salen molecules are found in two adsorption configurations, depicted in the inset in Figure 5(a) (upper left corner). One adsorption mode where the V(O)salen molecules are mobile (fuzzy streaks) during scanning and a second mode where the molecules are immobile residing on the protrusions of the Ag superstructure, hence steered by the Moiré template effect. The Ag-capped Co island (area B) are completely covered with molecules that are found to be hexagonally ordered. Also the pure Co islands (area C) are completely covered with molecules, but here the adsorption does not display any order. On the bilayer Ag layers (area D), V(O)salen does not adsorb, emphasizing that the bonding of the molecules on the Ag monolayer is stabilized by the more reactive Cu(111) substrate and the second Ag layer effectively decreases this interaction. At lower molecular coverages it is found that V(O)salen almost solely adsorbs on the pure Co islands (Area C), confirming that this is the most reactive surface towards adsorption of V(O)salen followed by the Ag-capped Co/Cu(111).

Adsorption of paramagnetic metal-organic complexes on ferromagnetic supports have proven to significantly alter

the electronic and magnetic properties of both surface and molecule.^{49–51} Even though direct adsorption of paramagnetic molecules onto a ferromagnet has proven to stabilize the magnetic moment of the central ion against thermal fluctuations, the proximity of the ion to the substrate results in a rigid coupling of the molecular moment to the magnetization of the substrate, making it challenging to control the magnetic state of the molecule independently.^{25,26} One successful route of stabilizing the molecular moment by a ferromagnetic substrate has been achieved by electronically decoupling the molecule from the surface, utilizing a passivating spacer layer of either graphene or insulating MgO. This has proven to both mediate the magnetic interaction between molecule and ferromagnet and additionally preserve the gas-phase electronic properties of the molecules, by hindering charge transfer from the surface.^{52–54} In addition to the patterned adsorption of V(O)salen on the Moiré structured Co and Ag/Co templates, the metallic Ag adlayer might impose an alternative to the aforementioned spacer layers, facilitating novel magnetic interactions between the Co sub-layer and the metal-organic molecules. In particular, the sandwich structure enables to study the Kondo physics of magnetic atoms and molecules, affected by the exchange interactions between said magnetic units and Co island.^{41,55} By this approach

the magnetic interaction is taking place in the third dimension, as opposed to the far more studied case of magnetic units interacting in the surface plane.^{56–59}

Conclusion

In conclusion, we have shown how V(O)salen, a potential molecular qubit candidate, adsorbs and assembles on a range of crystalline surfaces. On Ag(111) triangular nanostructures are observed, whereas the molecules form linear assemblies on Cu(111). Both cluster types follow the six-fold symmetry of the substrate. On Ag(111) the majority of molecules arrange in clusters, whereas on Cu(111) only 25 % of the molecules are found in clusters and the majority are isolated. We attribute this to a stronger molecule-substrate bonding on Cu(111) compared to Ag(111), that reduces the diffusivity and thus dominates over the intermolecular interaction governing the self-assembly.

On the modulated Co/Ag(111) and Ag/Co/Cu(111) surfaces, a regular patterned adsorption of the molecules is observed, steered by the strain-induced hexagonal Moiré superstructures. Molecules reside on the protrusions of the two textured templates, coinciding with a Co surface d -state being closest to E_F at these positions. This demonstrates how the surface reactivity can be controlled on the nanoscale and traced back to both geometrical and electronic effect. We hereby present an approach for patterned adsorption of molecules on ferromagnets achieved via Moiré superstructures in the surface. This is seldom the case for flat ferromagnetic surfaces as shown for V(O)salen adsorbing on Co islands grown on Cu(111), where the large surface reactivity leads to an unstructured adsorption and a partial dissociation of the molecules.

This way of engineering ferromagnetic surface might become an important strategy for developing molecular spintronics and integrating molecular qubits into larger quantum components.

Conflicts of interest

There are no conflicts to declare

Acknowledgements

The work was supported by the Danish National Committee for Research Infrastructure (NUFI) through the ESS-Lighthouse Q-MAT.

Notes and references

- 1 Y.-S. Ding, Y.-F. Deng and Y.-Z. Zheng, *Magnetochemistry*, 2016, **2**, 40.
- 2 J. M. Frost, K. L. Harriman and M. Murugesu, *Chemical Science*, 2016, **7**, 2470–2491.
- 3 A. Cornia and P. Seneor, *Nature Materials*, 2017, **16**, 505–506.
- 4 A. Urtizberea, E. Natividad, P. J. Alonso, M. A. Andrés, I. Gascón, M. Goldmann and O. Roubeau, *Advanced Functional Materials*, 2018, **28**, 1801695.
- 5 A. J. Heinrich, W. D. Oliver, L. M. K. Vandersypen, A. Ardavan, R. Sessoli, D. Loss, A. B. Jayich, J. Fernandez-Rossier, A. Laucht and A. Morello, *Nature Nanotechnology*, 2021, **16**, 1318–1329.
- 6 A. Chiesa, P. Santini, E. Garlatti, F. Luis and S. Carretta, *Reports on Progress in Physics*, 2024, **87**, 034501.
- 7 A. Urtizberea, E. Natividad, P. J. Alonso, L. Pérez-Martínez, M. A. Andrés, I. Gascón, I. Gimeno, F. Luis and O. Roubeau, *Materials Horizons*, 2020, **7**, 885–897.
- 8 D. Ranieri, F. Santanni, A. Privitera, A. Albino, E. Salvadori, M. Chiesa, F. Totti, L. Sorace and R. Sessoli, *Chemical Science*, 2023, **14**, 61–69.
- 9 C.-J. Yu, M. J. Graham, J. M. Zadrozny, J. Niklas, M. D. Krzyaniak, M. R. Wasielewski, O. G. Poluektov and D. E. Freedman, *J. Am Chem Soc*, 2016, **138**, 14678–14685.
- 10 L. Tesi, E. Lucaccini, I. Cimatti, M. Perfetti, M. Mannini, M. Atzori, E. Morra, M. Chiesa, A. Caneschi, L. Sorace and R. Sessoli, *Chemical Science*, 2016, **7**, 2074–2083.
- 11 T. Basova, V. Plyashkevich and A. Hassan, *Surface Science*, 2008, **602**, 2368–2372.
- 12 A. Yamashita, T. Maruno and T. Hayashi, *The Journal of Physical Chemistry*, 1993, **97**, 4567–4569.
- 13 J. V. Barth, *Annual Review of Physical Chemistry*, 2007, **58**, 375–407.
- 14 A. Kühnle, *Current Opinion in Colloid and Interface Science*, 2009, **14**, 157–168.
- 15 S. Stepanow, N. Lin and J. V. Barth, *Journal of Physics: Condensed Matter*, 2008, **20**, 184002.
- 16 S. Kuck, S.-H. Chang, J.-P. Klöckner, M. H. Prosenc, G. Hoffmann and R. Wiesendanger, *ChemPhysChem*, 2009, **10**, 2008–2011.
- 17 M. Bazarnik, B. Bugenhagen, M. Elsebach, E. Sierda, A. Frank, M. H. Prosenc and R. Wiesendanger, *Nano Letters*, 2016, **16**, 577–582.
- 18 M. Viciano-Chumillas, J. Jere, J. Hieulle, T. Mallah and F. Sully, *Journal of Physical Chemistry C*, 2012, **116**, 59.
- 19 M. Bazarnik, J. Brede, R. Decker and R. Wiesendanger, *ACS Nano*, 2013, **7**, 11341–11349.
- 20 S. Babiloliaei and L. Diekhöner, *Phys. Chem. Chem. Phys*, 2014, **16**, 11265.
- 21 T. G. Gopakumar, N. Néel, J. Kröger and R. Berndt, *Chemical Physics Letters*, 2009, **484**, 59–63.
- 22 J. Bork, P. Wahl, L. Diekhöner and K. Kern, *New Journal of Physics*, 2009, **11**, 113051.

- 23 J. Bork, J. Onsgaard and L. Diekhöner, *Journal of Physics: Condensed Matter*, 2010, **22**, 135005.
- 24 J. Bork, L. Diekhöner, Z. S. Li and J. Onsgaard, *Surface Science*, 2010, **604**, 1536.
- 25 C. Iacovita, M. V. Rastei, B. W. Heinrich, T. Brumme, J. Kortus, L. Limot and J. P. Bucher, *Physical Review Letters*, 2008, **101**, 116602.
- 26 J. Brede, N. Atodiresei, S. Kuck, P. L. Lazic, V. Caciuc, Y. Morikawa, G. Hoffmann, S. Blügel and R. Wiesendanger, *Phys. Rev. Lett.*, 2010, **105**, 047204.
- 27 L. Diekhöner, M. A. Schneider, A. N. Baranov, V. S. Stepanyuk, P. Bruno and K. Kern, *Phys. Rev. Lett.*, 2002, **90**, 236801.
- 28 M. V. Rastei, B. Heinrich, L. Limot, P. A. Ignatiev, V. S. Stepanyuk, P. Bruno and J. P. Bucher, *Phys. Rev. Lett.*, 2007, **99**, 246102.
- 29 J. E. Bickel, F. Meier, J. Brede, A. Kubetzka, K. Von Bergmann and R. Wiesendanger, *Phys. Rev. B.*, 2011, **84**, 54454.
- 30 J. Bendix, *Journal of the American Chemical Society*, 2003, **125**, 13348–13349.
- 31 D. Z. Gao, J. Grenz, M. B. Watkins, F. F. Canova, A. Schwarz, R. Wiesendanger and A. L. Shluger, *ACS Nano*, 2014, **8**, 5339–5351.
- 32 J. V. Barth, G. Costantini and K. Kern, *Nature*, 2005, **437**, 671–679.
- 33 C. Wang, J.-H. Yuan, G. Xie, M.-J. Yu and J. Li, *Acta Crystallographica Section E*, 2008, **64**, m775–m776.
- 34 K. Doi, E. Minamitani, S. Yamamoto, R. Arafune, Y. Yoshida, S. Watanabe and Y. Hasegawa, *Phys. Rev. B.*, 2015, **92**, 064421.
- 35 M. Mavrikakis, B. Hammer and J. K. Nørskov, *Phys. Rev. Lett.*, 1998, **81**, 2819–2822.
- 36 A. Nilsson, L. G. Pettersson, B. Hammer, T. Bligaard, C. H. Christensen and J. K. Nørskov, *Catalysis Letters*, 2005, **100**, 111–114.
- 37 Y. Saisyu, T. Hirahara, R. Hobara and S. Hasegawa, *Journal of Applied Physics*, 2011, **110**, 1755.
- 38 X. Chen and M. Alouani, *Physical Review B*, 2010, **82**, 094443.
- 39 S. Javaid, M. Bowen, S. Boukari, L. Joly, J.-B. Beaufrand, X. Chen, Y. J. Dappe, F. Scheurer, J.-P. Kappler, J. Arabski, W. Wulfhekel, M. Alouani and E. Beaurepaire, *Physical Review Letters*, 2010, **105**, 077201.
- 40 V. E. Campbell, M. Tonelli, I. Cimatti, J.-B. Moussy, L. Tortech, Y. J. Dappe, E. Rivière, R. Guillot, S. Delprat, R. Mattana, P. Seneor, P. Ohresser, F. Choueikani, E. Otero, F. Koprowiak, V. G. Chilkuri, N. Suaud, N. Guihéry, A. Galtayries, F. Miserque, M.-A. Arrio, P. Sainctavit and T. Mallah, *Nature Communications*, 2016, **7**, 13646.
- 41 O. O. Brovko, P. A. Ignatiev, V. S. Stepanyuk and P. Bruno, *Physical Review Letters*, 2008, **101**, 036809.
- 42 S. S. Letters, W. E. McMahon and E. S. Hirschorn, *Surface Science*, 1992, **279**, L231–L235.
- 43 B. Hammer and J. K. Nørskov, *Nature*, 1995, **376**, 238–240.
- 44 J. De La Figuera, J. E. Prieto, C. Ocal and R. Miranda, *Physical Review B*, 1993, **47**, 13043–13046.
- 45 N. N. Negulyaev, V. S. Stepanyuk, P. Bruno, L. Diekhöner, P. Wahl and K. Kern, *Physical Review B*, 2008, **77**, 125437.
- 46 M. Sicot, O. Kurnosikov, O. A. Adam, H. J. Swagten and B. Koopmans, *Physical Review B*, 2008, **77**, 035417.
- 47 J. Park, C. Park, M. Yoon and A. P. Li, *Nano Letters*, 2017, **17**, 292–298.
- 48 S. Gueddida, M. Gruber, T. Miyamachi, E. Beaurepaire, W. Wulfhekel and M. Alouani, *J. Phys. Chem. Lett.*, 2016, **7**, 900.
- 49 J. Brede, N. Atodiresei, V. Caciuc, M. Bazarnik, A. Al-Zubi, S. Blügel and R. Wiesendanger, *Nature Nanotechnology*, 2014, **9**, 1018–1023.
- 50 J. Schwöbel, Y. Fu, J. Brede, A. Dilullo, G. Hoffmann, S. Klyatskaya, M. Ruben and R. Wiesendanger, *Nature Communications*, 2012, **3**, 953.
- 51 C. Barraud, P. Seneor, R. Mattana, S. Fusil, K. Bouzehouane, C. Deranlot, P. Graziosi, L. Hueso, I. Bergenti, V. Dediu, F. Petroff and A. Fert, *Nature Physics*, 2010, **6**, 615–620.
- 52 S. Marocchi, A. Candini, D. Klar, W. Van Den Heuvel, H. Huang, F. Troiani, V. Corradini, R. Biagi, V. De Renzi, S. Klyatskaya, K. Kummer, N. B. Brookes, M. Ruben, H. Wende, U. Del Pennino, A. Soncini, M. Affronte and V. Bellini, *ACS Nano*, 2016, **10**, 9360.
- 53 M. Scardamaglia, S. Lisi, S. Lizzit, A. Baraldi, R. Larciprete, C. Mariani and M. G. Betti, *The Journal of Physical Chemistry C*, 2013, **117**, 3019–3027.
- 54 C. Wäckerlin, F. Donati, A. Singha, R. Baltic, S. Rusponi, K. Diller, F. Patthey, M. Pivetta, Y. Lan, S. Klyatskaya, M. Ruben, H. Brune and J. Dreiser, *Advanced Materials*, 2016, **28**, 5195–5199.
- 55 Y. H. Zhang, S. Kahle, T. Herden, C. Strohm, M. Mayor, U. Schlickum, M. Ternes, P. Wahl and K. Kern, *Nature Communications*, 2013, **4**, 2110.
- 56 N. Tsukahara, S. Shiraki, S. Itou, N. Ohta, N. Takagi and M. Kawai, *Physical Review Letters*, 2011, **106**, 187201.
- 57 P. Wahl, P. Simon, L. Diekhöner, V. S. Stepanyuk, P. Bruno, M. A. Schneider and K. Kern, *Physical Review*

Letters, 2007, **98**, 056601.

- 58 J. Girovsky, J. Nowakowski, M. E. Ali, M. Baljovic, H. R. Rossmann, T. Nijs, E. A. Aeby, S. Nowakowska, D. Siewert, G. Srivastava, C. Wäckerlin, J. Dreiser, S. Decurtins, S. X. Liu, P. M. Oppeneer, T. A. Jung and N. Ballav, *Nature Communications*, 2017, **8**, 15388.
- 59 A. A. Khajetoorians, J. Wiebe, B. Chilian and R. Wiesendanger, *Science*, 2011, **332**, 1062–1064.